On the Effect of a Point Mutation on the Reactivity of CuZn Superoxide Dismutase: A Theoretical Study

Andrea Amadei,*,† Maira D'Alessandro,†,‡ Maurizio Paci,† Alfredo Di Nola,‡ and Massimiliano Aschi§

Dipartimento di Scienze e Tecnologie Chimiche Università di Roma "Tor Vergata", Via della Ricerca Scientifica 1, 00133 Roma, Italy, Dipartimento di Chimica, Università di Roma "La Sapienza", P.le Aldo Moro 5, 00185 Roma, Italy, and Dipartimento di Chimica, Ingegneria Chimica e Materiali, Università degli studi dell'Aquila, via Vetoio, 67010 L'Aquila, Italy

Received: December 6, 2005; In Final Form: February 10, 2006

In this paper, we investigate the effects of a point mutation on the enzymatic activity of copper−zinc superoxide dismutase, which we recently studied in detail by means of a theoretical-computational procedure (*J. Phys. Chem. B* **2004**, *108*, 16255). Comparison of the reactivity of the initial catalytic steps in this mutant (G93A mutation far from the active site) with our previous data, reveals the beautiful mechanical-dynamical architecture of the enzyme, altered by such an apparently irrelevant mutation. Finally, our results suggest a possible atomic-molecular-based explanation for the mutant-pathology correlation, in line with the most recent experimental data.

1. Introduction

Despite the amazing advances in our knowledge on biological processes at molecular level, the detailed theoretical comprehension of enzyme reactions, or more in general of biochemical reactions within proteins, is still a largely untackled problem. This is essentially due to the tremendous physical-chemical complexity of such processes, which are then often described by phenomenological schemes as usual in biochemistry and molecular biology. Only in the past decade, because of improved computer power, several theoretical-computational attempts have been made to model enzymatic reactions, usually by means of a drastic simplification of the problem either studying the isolated reaction center (the chemical system treated quantum mechanically, i.e., the quantum center) or including its interaction with the environment via a macroscopic mean field approach, clearly oversimplifying the system. Alternatively, completely semiclassical models including Hamiltonian terms describing the reaction step of interest, have been used to treat the coupling of the chemical reaction with its molecular environment. Unfortunately the missing quantum mechanical treatment of the electronic reaction events typically makes these approaches not suitable for studying enzyme-like reactions.[2] However, from this growing body of theoretical-computational results, it emerged the important role exerted by the environment on the reaction center behavior,[3,10,12] hence leading to the need of mixed quantum-classical methods (e.g. QM/MM) aimed to explicitly include the environment, at atomic-molecular level, in the reaction modeling.[3−11] In this line we developed a theoretical-computational method, the perturbed matrix method (PMM),[13−18] based on the explicit treatment of the coupling between the environment atomic-molecular configurational fluctuations, as provided by full atomistic molecular dynamics (MD) simulations, with the electronic properties of a subpart of the complex system considered. PMM can be considered a mixed quantum-classical method. However, its use in the present paper as well as in the previous ones differs from typical QM/MM methods essentially for two aspects: first, in our approach, the dynamical-statistical sampling is achieved by using for the whole system an atomistic semiempirical Hamiltonian (i.e., no electronic wave function calculations are necessary to obtain the force field acting on the atoms); second, we obtain the electronic properties of the quantum center (QC) interacting with its environment (perturbed properties) via a quantum perturbation method requiring standard quantum chemical calculations only for a very limited set of QC atomic structures and providing, at each atomic configuration given by the dynamical-statistical sampling, the perturbed QC states as a function of the environment perturbing electric field. This allows the calculation of QC perturbed electronic properties and their coupling with atomic motions over a very extended configurational sampling. Very recently, such a procedure has been extended, by combining it with basic statistical mechanics, to treat chemical reactions occurring in complex molecular systems,[19] and its application to an enzymatic reaction, superoxide anion (O_2^-) disproportionation within copper−zinc superoxide dismutase (CuZnSOD), the reaction mechanism successfully clarified in detail.[1] The main result obtained in that paper was the essential role of the protein−solvent environment in determining the triggering step of the catalytic cycle: the electron transfer from superoxide to the copper that takes place only if the protein−solvent environment is present, as it provides a specific pattern of perturbing electric field fluctuations at the active site.[1] Such a reaction step, associated with a largely negative free energy change and determined by the simultaneous superoxide oxidation and His63−copper bond disruption,[1] is also very efficient, as no transition state was found by our calculations, in agreement with the experimentally observed

* To whom correspondence should be addressed. E-mail: andrea.amadei@uniroma2.it (A.A.); m.aschi@caspur.it (M.A.).

† Dipartimento di Scienze e Tecnologie Chimiche Università di Roma "Tor Vergata".

‡ Dipartimento di Chimica, Università di Roma "La Sapienza".

§ Dipartimento di Chimica, Ingegneria Chimica e Materiali, Università degli Studi dell'Aquila.

10.1021/jp057095h CCC: $33.50
Published on Web 03/18/2006

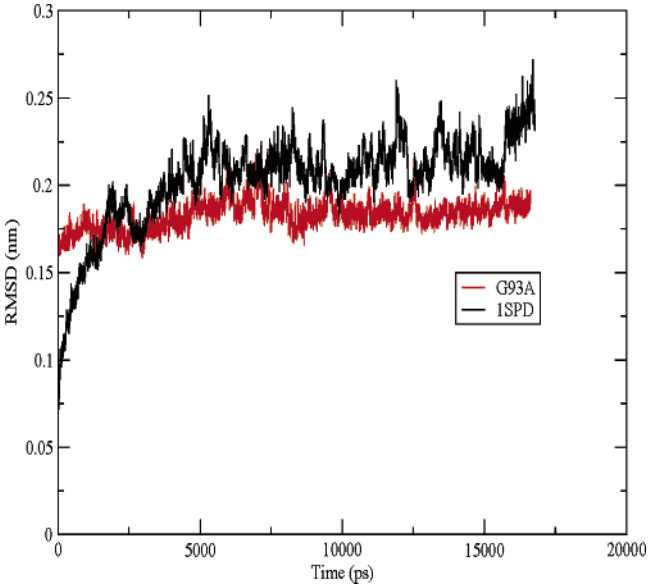

Figure 1. RMSD of G93A and wild type (1SPD) as a function of the simulation time. Note that, for the wild type, the reference structure is the energy-minimized crystal structure, while for G93A, the reference structure is the initial MD structure obtained by a configuration of the wild-type simulation, substituting Gly93 with Ala.

diffusion rate-limited kinetics.[34] Remarkably, no accessible conformational region of the folded protein, in our simulation, was able to significantly inhibit this reaction step.[1] These results pointed out the great importance of the mechanical-dynamical protein organization, designed to generate a well-defined electric field pattern at the reaction center, suggesting that even a point mutation far from the active site could have a dramatic effect on the reactivity. In this paper, we study, with the same theoretical-computational procedure, the G93A mutant associated with a pathological condition[20] (amyotrophic lateral sclerosis), comparing its reaction behavior with our previous results. Such a comparison further clarifies the determinants of the enzymatic activity emerging from the structural-dynamical protein organization and suggests an atomic-molecular explanation for the mutant involvement into the pathology, based on an altered conformational-reactivity behavior, which seems in agreement with the experimentally observed oxidative damage of the mutant itself.[20]

All the details about the theoretical and computational procedures used in this article are described in previous papers[1,19] and summarized in the Methods Section.

2. Methods

The 300 K MD simulation of G93A in water to study the mutant reaction has been performed identically to the simulation utilized to study the wild-type reaction,[1] except for the initial MD configuration, which was obtained by substituting Gly93 with Ala in a configuration provided by the simulation used in the previous article. This was necessary as, unlike the wild type,[21] no G93A crystal structure is available. The total G93A simulation time length used in the reactivity calculations was 16 ns, identical to the time length used for the wild type, and in Figure 1, we show, via the time dependence of the root-mean-square deviation (RMSD) from the initial MD mutant structure, the stability of G93A, demonstrating the absence of partial unfolding in our simulation. Note that the initial fast G93A relaxation occurring in the equilibration run is not present in the figure, as for this mutant we show the RMSD of the productive run only. The detailed description of the PMM model for chemical reactions is given in the previous paper.[19] Here, we only provide a summary of the main relations used to model CuZnSOD reaction. Briefly, the perturbed QC Hamiltonian matrix $\tilde{H}$ on the Born−Oppenheimer (BO) surface is

$$\tilde{H} \cong \tilde{H}^{\circ} + q_T \mathscr{V} \tilde{I} + \tilde{Z}_1 + \Delta V \tilde{I} \tag{1}$$

where $\tilde{H}^{\circ}$ is the unperturbed QC Hamiltonian matrix constructed via configuration interaction calculations with single and double excitations (CISD), including the ground state plus seven excited states,[1] q_T is the QC total charge, $\mathscr{V}$ is the perturbation electric potential exerted by the environment on the quantum center, $\tilde{Z}_1$ is the perturbation matrix provided by the inner products between the unperturbed transition dipoles and the perturbing electric field, and ΔV approximates the perturbation due to all the terms from the quadrupoles on as a simple short-range potential. It is worth noting that, at each MD frame, the electric potential and field exerted by the environment can be calculated and the perturbed Hamiltonian matrix diagonalized. Hence, a trajectory of the perturbed eigenvalues and eigenvectors is obtained. Such a calculation, if carried out along predefined reaction coordinates, provides the free energy change (ΔA) and the related electronic properties (e.g., the ground-state dipole $\langle \boldsymbol{\mu}_{0,0} \rangle_b$) at a generic point $\boldsymbol{\eta}_b$ of the reaction coordinates[19]

$$\Delta A \cong -kT \ln \langle e^{-\beta \Delta(\epsilon' + q_T \mathscr{V})} \rangle^0_{\boldsymbol{\eta}_a} \tag{2}$$

$$\langle \boldsymbol{\mu}_{0,0} \rangle_b \cong \frac{\langle e^{-\beta \Delta(\epsilon' + q_T \mathscr{V})} \boldsymbol{\mu}_{0,0} \rangle^0_{\boldsymbol{\eta}_a}}{\langle e^{-\beta \Delta(\epsilon' + q_T \mathscr{V})} \rangle^0_{\boldsymbol{\eta}_a}} \tag{3}$$

In the previous equations, ϵ' is the eigenvalue of the perturbation matrix $\tilde{Z}_1$, $\Delta(\epsilon' + q_T \mathscr{V})$ provides the energy change, for each MD frame, due to the transition along the reaction coordinates, and $\boldsymbol{\eta}_a$ is the position of the reaction coordinates used to obtain the statistical ensemble, i.e., used in the MD simulation. Moreover, the subscript $\boldsymbol{\eta}_a$ and the zero superscript of the averaging operator means that the average is taken in the statistical ensemble where the reaction coordinates are constrained at $\boldsymbol{\eta}_a$, with the quantum center in its ground vibrational state. The perturbed ground-state dipole $\boldsymbol{\mu}_{0,0}$ is evaluated by PMM via the perturbed Hamiltonian eigenvectors set $\boldsymbol{c}_i$ from[16] $\boldsymbol{\mu}_{i,j} = \langle \Phi_i | \hat{\boldsymbol{\mu}} | \Phi_j \rangle$,

$$\boldsymbol{\mu}_{i,j} = \boldsymbol{c}_i^{*T} \tilde{\Lambda}_x^0 \boldsymbol{c}_j \, \boldsymbol{i} + \boldsymbol{c}_i^{*T} \tilde{\Lambda}_y^0 \boldsymbol{c}_j \, \boldsymbol{j} + \boldsymbol{c}_i^{*T} \tilde{\Lambda}_z^0 \boldsymbol{c}_j \, \boldsymbol{k} \tag{4}$$

$$[\tilde{\Lambda}_x^0]_{l,l'} = \langle \Phi_l^0 | \hat{\mu}_x | \Phi_{l'}^0 \rangle \tag{5}$$

$$[\tilde{\Lambda}_y^0]_{l,l'} = \langle \Phi_l^0 | \hat{\mu}_y | \Phi_{l'}^0 \rangle \tag{6}$$

$$[\tilde{\Lambda}_z^0]_{l,l'} = \langle \Phi_l^0 | \hat{\mu}_z | \Phi_{l'}^0 \rangle \tag{7}$$

where, obviously, Φ, Φ^0 are the perturbed and unperturbed Hamiltonian eigenfunction, respectively, $\hat{\boldsymbol{\mu}}$ is the dipole operator, and $\boldsymbol{c}^{*T}$ is the transposition of the complex conjugated of $\boldsymbol{c}$ (typically, from quantum-chemical calculations, $\tilde{H}$ has only real elements, and hence, $\boldsymbol{c} = \boldsymbol{c}^*$ is a real eigenvector). Note that the use of a frozen quantum center, except for the reaction coordinates considered, is not at all required by our approach[14,19] but allows a simple and reliable PMM application when we deal with rigid or semirigid quantum centers. The perturbing electric field, used to construct the perturbed Hamiltonian matrix utilized in PMM, was obtained at each MD configuration by the atomic charges within the silmulation box (excluding QC charges).

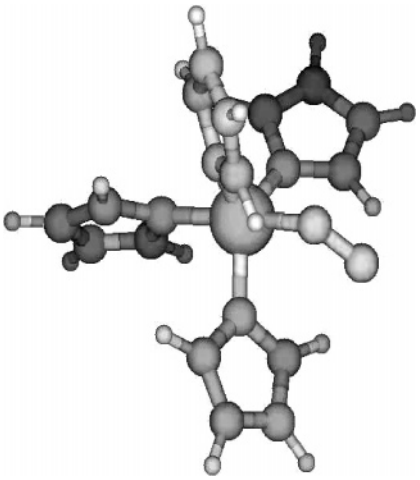

Figure 2. Picture of the quantum center (CHS) we used.

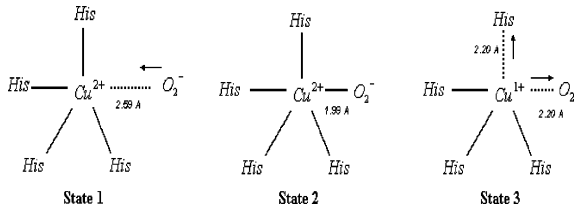

Figure 3. Schematic view of the three chemical states.

We utilized the same reaction center, the quantum center, of the previous article, defined by the copper atom, its four coordinating histidine side chains, and the bound superoxide (see Figure 2), hereafter defined as CHS. To schematize the first part of the enzymatic reaction, i.e., the superoxide oxidation (see eq 9), we employed the three chemical states (Figure 3), introduced in the previous paper, and defined by the following CHS geometries: $Cu-O_2^-$ bond heavily stretched, 2.6 Å, state 1 (CS1); CHS in the $Cu-O_2^-$ binding minimum free energy condition, $Cu-O_2^-$ bond at 1.995 Å, state 2 (CS2); Cu−O and His63−Cu bonds initially stretched, both at 2.2 Å, state 3 (CS3). Moreover, following the previous article, we need to define the residual dipole along a given chemical bond involving the copper. This observable describes the changes of CHS electron density in the direction of the chemical bond and is obtained via

$$\Delta\mu = (\boldsymbol{\mu} - \boldsymbol{\mu}_{\mathrm{ref}})\cdot\boldsymbol{\xi} \tag{8}$$

where $\boldsymbol{\mu} = \langle\boldsymbol{\mu}_{0,0}\rangle_{\mathrm{b}}$ is the actual CHS electric dipole at a given $\boldsymbol{\eta}_{\mathrm{b}}$ position of the reaction coordinates, $\boldsymbol{\mu}_{\mathrm{ref}}$ is the dipole at the same position of the reaction coordinates, obtained by using the unperturbed charge density at a reference condition (chemical state 1 for the isolated CHS), and $\boldsymbol{\xi}$ is the unit vector defining the chosen chemical bond direction. Hence, $\Delta\mu$ provides a direct measure of the non trivial charge density modification involved in the electron transfer, obtained with respect to the unperturbed reference charge distribution (about −0.6 au for the superoxide ion): $\Delta\mu < 0$ implies an electron flux from the copper, while $\Delta\mu > 0$ provides an electron flux toward the copper.

3. Results and Discussion

Copper−zinc superoxide dismutase is a homodimeric protein[22−24] that catalyzes the superoxide anion (O_2^-) disproportionation, described by the chemical scheme

$$Cu^{2+} + O_2^- \rightarrow Cu^+ + O_2 \tag{9}$$

$$Cu^+ + O_2^- + 2H^+ \rightarrow H_2O_2 + Cu^{2+} \tag{10}$$

Each subunit contains one copper (Cu) and one zinc (Zn) atom. The Cu is coordinated to four histidines, forming a distorted square planar geometry.[23] One of these histidines (His63) formally exhibits a negative charge and acts as a bridge between Cu and Zn.[24] The role of these atoms is known to be substantially different. The Zn atom does not directly participate to the catalytic process and has a structural stabilization role,[24] while Cu plays an essential role in the enzymatic catalysis.[22] According to experimental evidences,[22,24−34] in the first part of the reaction, O_2^- is oxidized by Cu^{2+} to molecular oxygen (O_2) (eq 9), and subsequently (eq 10), a second superoxide anion is reduced by Cu^+ to produce hydrogen peroxide. In this mechanistic scheme,[29] one of the crucial steps is the concerted Cu−His63 coordination bond disruption and superoxide oxidation which, from our previous study,[1] occurs only when the reaction center (the quantum center, CHS, shown in Figure 2) is interacting with its protein−solvent environment. The mutant chosen, G93A, given by a Gly → Ala point mutation far from the active site (see Figure 4), is involved in a severe degenerative disease of motor neurons, amyotrophic lateral sclerosis (ALS). Interestingly, G93A is not characterized by an altered metal−protein binding affinity, showing an enzymatic activity rather close to the wild type,[20] and our simulations clearly indicate that G93A and the wild type (1SPD) have very similar overall structures with virtually identical secondary structure elements (data not shown). However, such a mutant somehow promotes oxidative damages which strikingly largely involve the mutant itself, suggesting a possible self-oxidative activity[20] essentially absent in the wild type. As described in the Methods Section, we schematize the first reaction steps via three chemical states, CS1, CS2, and CS3, shown in Figure 3, defining three conditions of the reaction center (CHS). In Figure 5, we show the reaction (Helmholtz) free energy for both 1SPD and G93A as a function of the three chemical states (we used CS2 as the reference state, i.e., the zero of the free energy). This figure clearly shows that, although in both proteins the CS1 → CS2 → CS3 reaction occurs with a large free energy decrease, for G93A, a very relevant increase of the free energy in CS3 (about 40 kJ/mol) is present, implying a rather different perturbation pattern at the reaction center. In the figure, the unperturbed reaction free energy is also shown (obtained for the isolated CHS), clearly showing the essential role of the protein in the reaction. It is worth noting that, although for both simulations, the reaction free energies obtained might be not fully converged, the estimated 40 kJ/mol variation in the free energy change associated with the CS2 → CS3 transition clearly indicates a relevant increase of the $[CS2]_{eq}/[CS3]_{eq}$ equilibrium constant (at 300 K for 40 kJ/mol variation about 10^7 times), thus indicating a much higher equilibrium density of CS2 in G93A. To investigate such a relevant modification in the reaction between 1SPD and G93A, we considered the residual dipole along all the copper chemical bonds. This property $\Delta\mu$ provides a direct measure of the nontrivial CHS charge density modification, along a given chemical bond, involved in the electron transfer, and it is obtained with respect to the unperturbed reference charge distribution (about −0.6 au for the superoxide ion, see Methods). In Figures 6 and 7, we show the residual dipole for two chemical bonds that resulted as the most relevant in the reaction electron density rearragement: the $Cu-O_2^-$ and Cu−His48 bonds. In

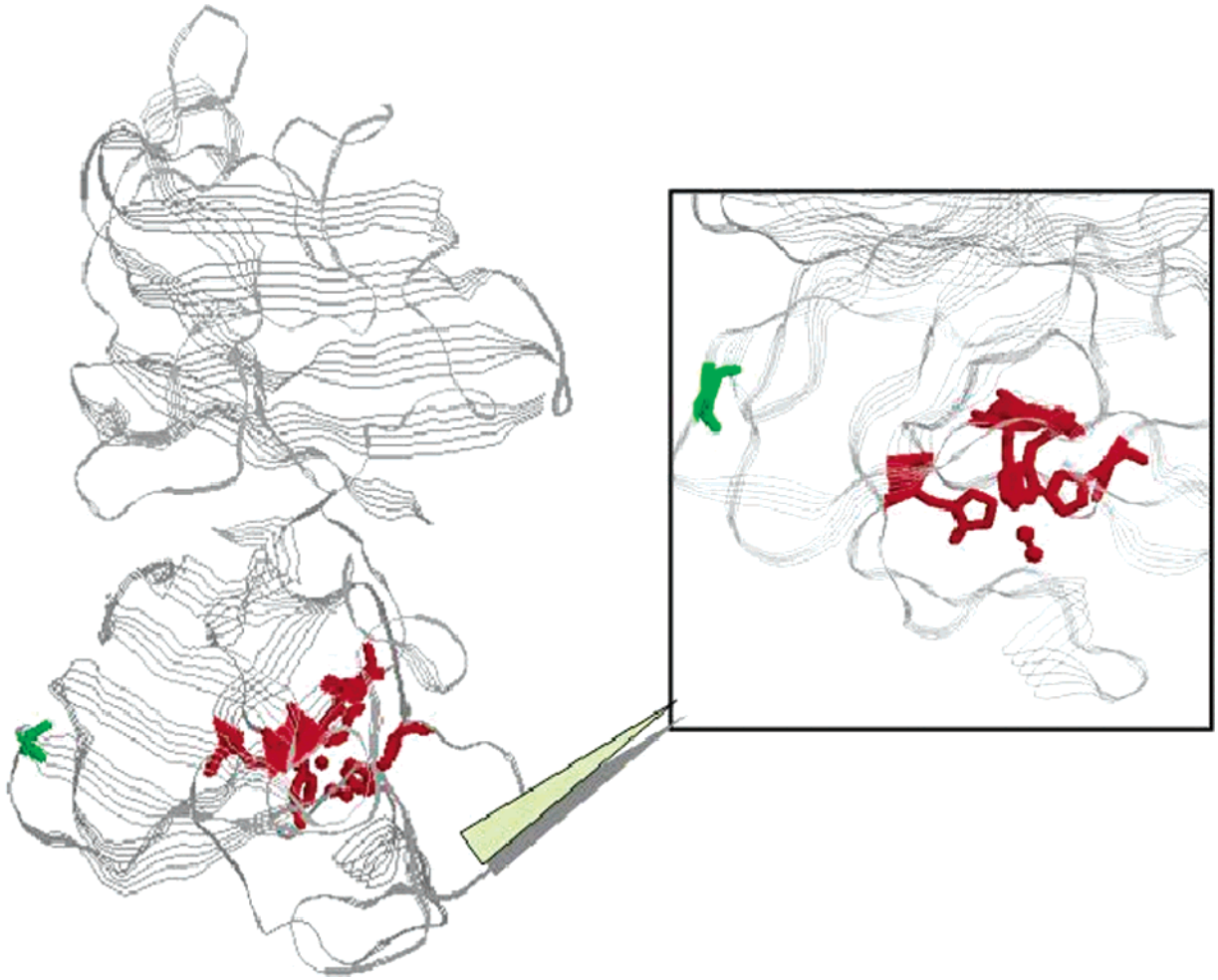

Figure 4. Three-dimensional structure of the wild type showing the relative position of the reaction center (CHS) in red and the mutation residue (Gly93) in green.

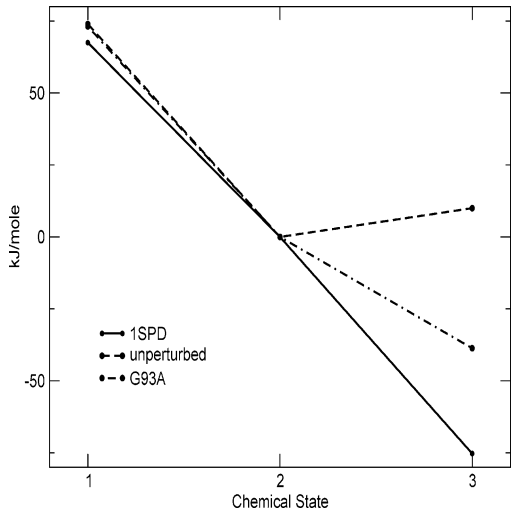

Figure 5. Reaction free energy for both 1SPD and G93A as a function of the three chemical states (we used CS2 as the reference state, i.e., the zero of the free energy): unperturbed CHS = dashed line, perturbed 1SPD CHS = solid line, perturbed G93A CHS = dashed−dotted line.

Figure 6, we show the 1SPD residual dipoles, and in Figure 7, the G93A ones, for the three chemical states defined. It is evident from the figures the equivalence for both proteins of the Cu−O_2^- residual dipole, indicating in the third chemical state the complete superoxide to copper electron transfer, i.e., 2.6−2.7 au equivalent to 0.6−0.7 electrons (the reference superoxide electronic excess) moving from superoxide to copper.[1] On the

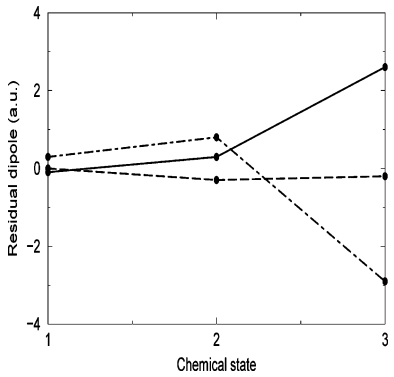

Figure 6. Three states residual dipoles along Cu−O_2^- and Cu−His48 bonds in 1SPD enzyme: Cu−O_2^- residual dipole in the unperturbed CHS = dashed line, Cu−O_2^- residual dipole in the perturbed CHS = solid line, Cu−His48 residual dipole in the perturbed CHS = dashed−dotted line.

contrary, the residual dipole along the Cu−His48 bond clearly shows a difference: in 1SPD, an almost specular electron transfer occurs, moving 0.7−0.8 electrons from copper to the histidine nitrogen, showing that the electronic current involved in the reaction is flowing actually from superoxide to histidine 48; in G93A, such a latter electron transfer, although still present, is reduced corresponding only to about 0.4 electrons moving from copper to histidine 48. Such a difference, clearly associated with the large reaction free energy variation observed in CS3, is due to the change of the perturbing electric field

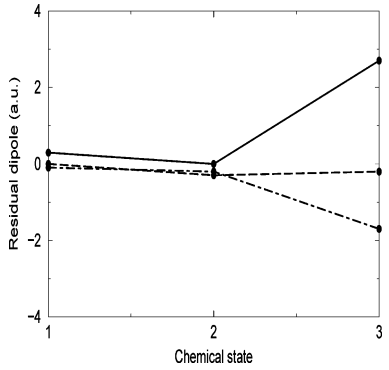

Figure 7. Three states residual dipoles along $Cu-O_2^-$ and Cu−His48 bonds in G93A enzyme: $Cu-O_2^-$ residual dipole in the unperturbed CHS = dashed line, $Cu-O_2^-$ residual dipole in the perturbed CHS = solid line, Cu−His48 residual dipole in the perturbed CHS = dashed−dotted line.

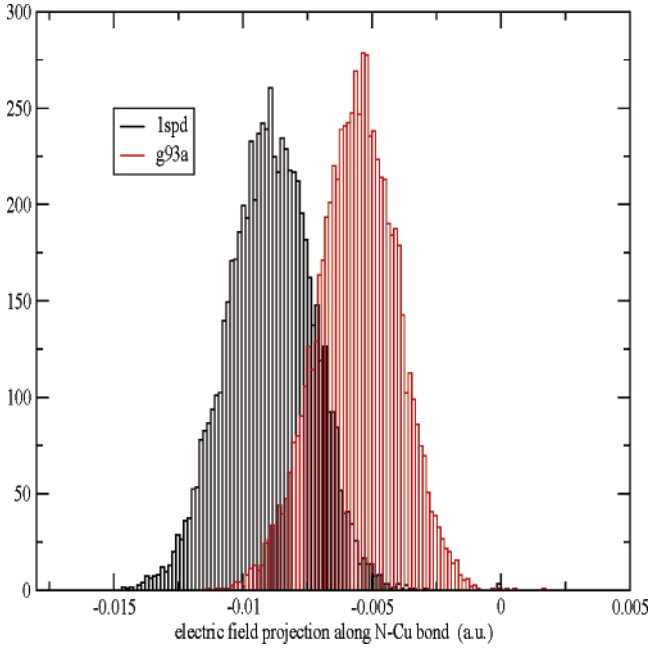

Figure 8. Normalized histogram of the electric field (au) projection along the Cu−His48 bond, for G93A (red) and 1SPD (black).

pattern at CHS, Figures 8 and 9, caused by the changes in the conformational fluctuation pattern induced by the point mutation. Note that, in Figures 6 and 7, we also provide the unperturbed $Cu-O_2^-$ residual dipole, clearly indicating that no electron transfer occurs in the isolated reaction center, as shown in the previous paper. To pinpoint the possible residues mainly responsible for the G93A−1SPD perturbing electric field modification (essentially the electric field component along Cu−His48 bond), we analyzed the residue contribution to the perturbing electric field.[1] In Figure 10, we show the variation of the average electric field projection along the Cu−His48 bond for each residue, as obtained by subtracting the wild-type values from the mutant ones. This figure clearly indicates the presence of a limited set of key residues responsible for the modification of the perturbing field. Note that the positive peaks indicate residues inhibiting the Cu−His48 electron flux, while negative ones correspond to enhancing residues. Interestingly, among the residues providing the largest peaks in the previous figure (essentially charged residues close to the reaction center), only Arg143 undergoes a relevant dynamical variation of its contribution to the perturbing electric field. This is shown in Figure 11, where we report the variation of the fluctuation (standard

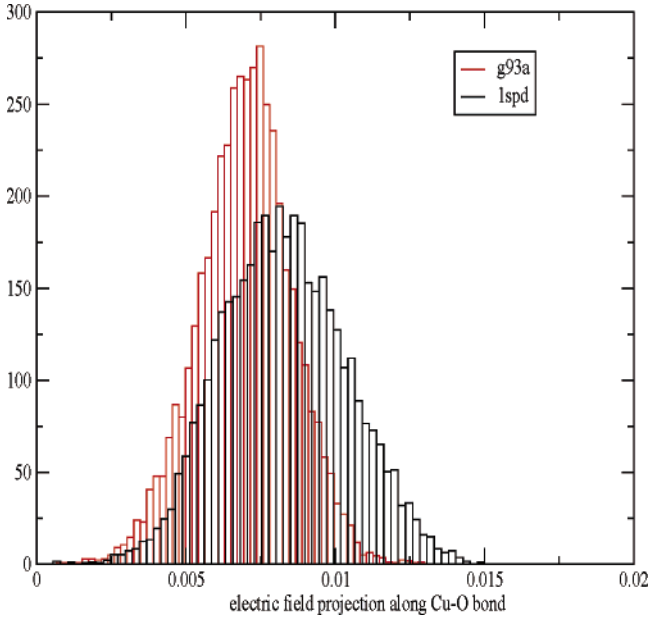

Figure 9. Normalized histogram of the electric field (au) projection along the Cu−superoxide bond, for G93A (red) and 1SPD (black).

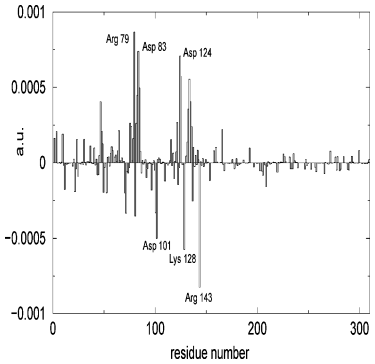

Figure 10. Variation of the average electric field (per residue) projection along the Cu−His48 bond, as obtained by subtracting the wild-type values from the mutant ones.

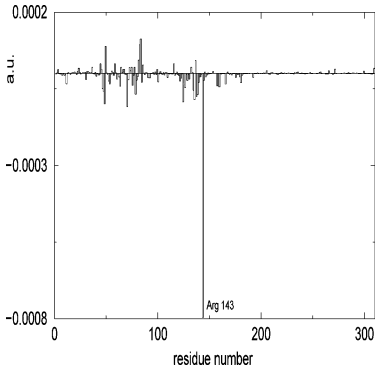

Figure 11. Variation of the fluctuation (standard deviation) of the electric field (per residue) projection along the Cu−His48 bond, as obtained by subtracting the wild-type values from the mutant ones.

deviation) of the electric field projection along the Cu−His48 bond for each residue, as obtained by subtracting the wild-type values from the mutant ones. It is to be noted that, in G93A, the Arg143 electric field fluctuation is largely reduced (large negative peak) as a consequence of a drastic reduction of its side chain mobility. The last figures indicate that the main effects produced by the point mutation are: a variation of the average relative orientation of the reaction center (CHS) and a set of key residues, and an increased rigidity of Arg143 side chain.

Such data clearly show that G93A mutation results in a subtle combination of static (structural) and fluctuation effects modifying the main contributions to the perturbing electric field pattern.

Finally, considering that the transition from state 2 to state 3 is very fast (a rough estimate at 300 K based on a diffusive model over the energy surfaces provides a subpicosecond kinetics), we may describe the reaction main paths for the first part of the catalytic cycle via the simple kinetic scheme

$$E{-}O_2^- \rightleftharpoons E{\cdots}O_2 \rightarrow E + O_2 \quad (11)$$

$$E{-}O_2^- \rightarrow E' \quad (12)$$

where E is the enzyme, $E{-}O_2^-$ is the covalent complex (our chemical state 2), $E{\cdots}O_2$ indicates an intermediate molecular complex defined by the Cu−O and Cu−His63 bonds just broken, with the molecular oxygen still close to the copper (essentially a chemical state a bit beyond our chemical state 3), and E′ represents the possible oxidatively damaged enzyme due to the reactivity of the bound superoxide. Note also that the $E{-}O_2^- \rightleftharpoons E{\cdots}O_2$ interconversion may be considered as instantaneously equilibrated or providing a steady state for the intermediate complex during the $E{\cdots}O_2 \rightarrow E + O_2$ and $E{-}O_2^- \rightarrow E'$ relaxations. Within such a kinetic scheme, we may approximate the rates of the previous reactions as

$$[\dot{O}_2] \cong k[E{\cdots}O_2] \quad (13)$$

$$[\dot{E}'] \cong k'K_{eq}[E{\cdots}O_2] \quad (14)$$

$$K_{eq} = \frac{[E{-}O_2^-]_{eq}}{[E{\cdots}O_2]_{eq}} \quad (15)$$

where k, k' are the rate constants for the $E{\cdots}O_2 \rightarrow E + O_2$ and $E{-}O_2^- \rightarrow E'$ transitions, respectively, for the latter, possibly including a steady state correction. A good measure of the kinetic balance between the productive reaction forming molecular oxygen and the oxidative damages produced by the bound superoxide is given by

$$\chi = \frac{[\dot{E}']}{[\dot{O}_2]} \cong \frac{k'}{k}K_{eq} \quad (16)$$

which can be used to compare different CuZnSOD forms. In the present case, assuming that k, k' rate constants are basically the same for G93A and 1SPD and using the ratio of the $[CS2]_{eq}/[CS3]_{eq}$ equilibrium constants of these two proteins as obtained by the 40 kJ/mol CS2 → CS3 reaction free energy variation, we may write $\chi_{G93A}/\chi_{1SPD} \cong 10^7$ (1SPD and G93A subscripts clearly indicate that the property is referred to the corresponding enzyme type). Hence, although in the wild-type enzyme, a negligible equilibrium density of the covalent complex is present and then virtually no oxidative side reactions occur; in the G93A mutant where χ largely increases, we may well hypothesize a significant rate for these side oxidative damages due to the bound superoxide, eventually leading to the complete enzyme inactivation.

4. Conclusions

In this paper, we showed how the use of an advanced theoretical-computational procedure based on mixed quantum-classical calculations may shed light into the intimate behavior of enzyme reactions. We considered as a prototypical example the superoxide oxidation in CuZnSOD, i.e., the first part of the catalytic cycle. Comparison of the reactivity between the wild type and the G93A mutant, involved in the ALS pathology, further shows that the mechanical-dynamical protein architecture is designed to provide a specific perturbing electric field pattern at the active site. Such a perturbation pattern may be considered as one of the main determinants of the enzyme biochemical activity. Moreover, the results presented in this paper suggest a possible atomic-molecular-based explanation for the pathology mechanism induced by the G93A mutant: the apparently irrelevant G93A point mutation augments the stability of the bound superoxide (the covalent complex), providing a large rate increase of the possible oxidative damages due to the bound superoxide. Such damaging reactions, kinetically negligible in the wild-type enzyme, might well explain the experimentally observed G93A oxidation, eventually leading to the complete enzyme inactivation.

Acknowledgment. M. D'Alessandro and A. Di Nola acknowledge MIUR-PRIN 2003 "Structure and Dynamics of Redox Proteins" for financial support. Caspur-Roma and "Centro Ricerche e Studi Enrico Fermi" (Roma) are acknowledged for computational support. Finally, Dr. Isabella Daidone is acknowledged for the support given in the use of specific routines for kinetic calculations.

References and Notes

(1) D'Alessandro, M.; Aschi, M.; Paci, M.; Di Nola, A.; Amadei, A. *J. Phys. Chem. B.* **2004**, *108*, 16255.

(2) van den Bosch, M.; Swart, M.; Snijderst, J. G.; Berendsen, H. J. C.; Mark, A. E.; Oostenbrink, C.; van Gunsteren, W. F.; Canters, G. W. *ChemBioChem* **2005**, *6*, 738−746.

(3) Straib, M.; Hong, G.; Warshel, A. *J. Phys. Chem. B.* **2002**, *106*, 13333.

(4) Gao, J.; Thompson, M. A. *Combined Quantum Mechanical and Molecular Mechanical Methods*; ACS Symposium Series 712; American Chemical Society: Washington, DC, 1998.

(5) Sherwood, P. *Modern Methods and Algorithms of Quantum Chemistry*; Grotendorst, J., Ed.; NIC-Directors: Princeton, 2000; Vol. 3.

(6) Hillier, I. *THEOCHEM* **1999**, *463*, 45.

(7) Aaqvist, J.; Warshel, A. *Chem. Rev.* **1993**, *93*, 2523.

(8) Monard, G.; Merz. K. M. *Acc. Chem. Res.* **1999**, *32*, 904.

(9) Truhlar, D. G.; Gao, J.; Alhambra, C.; Garcia-Viloca, M.; Corchado, J.; Sanchez, M. L.; Villa, J. *Acc. Chem. Res.* **2002**, *35*, 341.

(10) Garcia-Viloca, M.; Gao, J.; Karplus, M.; Truhlar, D. G. *Science* **2004**, *303*, 186.

(11) Morokuma, K. *Philos. Trans. R. Soc. London, Ser. A* **2002**, *360*, 1149.

(12) Carloni, P.; Blochl, P. E.; Parrinello, M. *J. Phys. Chem.* **1995**, *99*, 1338.

(13) Aschi, M.; Spezia, R.; Di Nola, A.; Amadei, A. *Chem. Phys. Lett.* **2001**, *344*, 374.

(14) Spezia, R.; Aschi, M.; Di Nola, A.; Amadei, A. *Chem. Phys. Lett.* **2002**, *365*, 450.

(15) Spezia, R.; Aschi, M.; Di Nola, A.; Valentin, M. D.; Carbonera, D.; Amadei, A. *Biophys. J.* **2003**, *84*, 2805.

(16) Amadei, A.; Zazza, C.; D'Abramo, M.; Aschi, M. *Chem. Phys. Lett.* **2003**, *381*, 187.

(17) Aschi, M.; Zazza, C.; Spezia, R.; Bossa, C.; Di Nola, A.; Paci, M.; Amadei, A. *J. Comput. Chem.* **2004**, *25*, 974.

(18) Aschi, M.; D'Abramo, M.; Di Teodoro, C.; Di Nola, A.; Amadei, A. *ChemPhysChem* **2005**, *6*, 53.

(19) Amadei, A.; D'Alessandro, M.; Aschi, M. *J. Phys. Chem. B* **2004**, *108*, 16250.

(20) Valentine, J. S.; Hart, P. J. *Proc. Natl. Acad. Sci. U.S.A.* **2003**, *100*, 3617.

(21) Deng, H. X.; Hentati, A.; Tainer, J. A.; Iqbel, Z.; Cayabyab, A.; Hung, W. Y.; Getzoff, E. D.; Hu, P. et al. *Science* **1993**, *261*, 1047.

(22) McCord, J. M.; Fridovich S. J. *J. Biol. Chem.* **1969**, *241*, 6049.

(23) Tainer, J. A.; Gelzoff, E. D.; Beem, K. F.; Richardson, J. S.; Richardson, D. C. *J. Mol. Biol.* **1982**, *160*, 181.

(24) Strothkamp, K. G.; Lippard, S. J. *Acc. Chem. Res.* **1982**, *15*, 318.

(25) Weinstein, J.; Bielski, B. H. *J. Am. Chem. Soc.* **1980**, *102*, 4916.

(26) Tainer, J. A.; Getzoff, E. D.; Richardson, J. S.; Richardson, D. C. *Nature* **1983**, *396*, 284.

(27) Fielden, E. M.; Roberts, P. B.; Bray, R. C.; Lowe, D. J.; Mautner, G. N.; Rotilio, G.; Calabrese, L. *Biochem. J.* **1974**, *139*, 49.
(28) Klugh Hoth, D.; Fridovich, S. J.; Rabani, J. *J. Am. Chem. Soc.* **1973**, *95*, 2786.
(29) Hart, J. P.; Balbirnie, M. M.; Ogihara, N. L.; Nersissian, A. M.; Weiss, M. S.; Valentine, J. S.; Eisenberg, D. *Biochemistry* **1999**, *38*, 2167.
(30) Bertini, I.; Luchinat, C.; Monnanni, R. *J. Am. Chem. Soc.* **1985**, *107*, 2178.
(31) Blackburn, N. J.; Hasnain, S. S.; Binsted, N.; Diakun, G. P.; Garner, C. D.; Knowles, P. F. *Biochem. J.* **1984**, *219*, 985.
(32) Ogihara, N. L.; Parge, H. E.; Hart, P. J.; Weiss, M. S.; Goto, J. J.; Crane, B. R.; Tsang, J.; Slater, K.; Roe, J. A.; Valentine, J. S.; Eisenberg, D.; Tainer, J. A. *Biochemistry* **1996**, *35*, 2316.
(33) Murphy, L. M.; Strange, R. W.; Hasnain, S. S. *Structure* **1997**, *5*, 371.
(34) Fee, J. A.; Bull, C. *J. Biol. Chem.* **1986**, *261*, 13000.